

Biphoton bound state right above e-p pair birth threshold

Daniel L. Miller

Intel IDC4, M.T.M. Industrial, POB 1659, Haifa, Israel

In this letter, a biphoton state of matter that is an instant interplay between electromagnetic energy and electron-positron pairs is reported. The biphoton ladder diagram right above the $e-p$ pair birth threshold is summed up. Only one ladder diagram is most relevant, and the obtained propagator has a diffusion pole, with the diffusion coefficient expressed as $D \sim \alpha^{-2} \hbar/m \sim 2 \times 10^4 \text{cm}^2/\text{s}$, where α is the fine-structure constant and m is the electron mass. This diffusion coefficient, dependent only on fundamental constants, can describe an observable macroscopic object, for example, ball lightning. This is a realization of an object with oscillation of energy between an electromagnetic field and an $e-p$ pair. The energy is preserved, but the momentum is getting randomized. This continuous oscillation holds energy localized in space, expanding relatively slowly following the diffusion equation.

PACS numbers: 03.70.+k, 11.10.-z

This letter presents a discussion on photon-photon interaction and the conversion of electromagnetic energy to matter and back to photons. The reversible and periodic transition of energy between two forms is the most fundamental process in physics, seen as waves and pendulums. One-way transitions of energy from light to matter, for example, the Big Bang, and from matter to light, for example, positron emission tomography, are well studied. However, there is no discussion available on the process that occurs during such periodic transitions in a system.

Recent interest in the scattering of light by light (for recent reviews, please see [1, 2]) has been generated owing to the problems of the transparency of the universe and limitations on the intensity of high-power lasers [3]. Besides, experimentalists reported progress with observation of the birefringent vacuum[4] and the direct measurements of the light by light scattering cross section by the CMS experiment at the LHC[5].

The background microwave radiation uniformly fills the universe and causes scattering of passing photons owing to photon-photon interaction. The transparency of the universe, therefore, depends on the photon-photon scattering cross section. In second problem, the large number of photons produced by a super-strong laser interact among themselves. This interaction creates an avalanche-like cascade of copious electron and positron $e-p$ pairs; they, in turn, deplete the incoming laser pulse. In third problem, nonlinear terms known as Euler, Heisenberg, and Weisskopf Lagrangian makes index of refraction variable and dependent on polarization of a light beam in external magnetic and/or electric field.

The photon-photon scattering amplitude becomes imaginary right above the $e-p$ pair birth threshold [6]§127 when the energy of the photons $\hbar\omega$ is sufficient for the creation of an $e-p$ pair, $2\hbar\omega \geq 2mc^2$. This indicates energy transfer from the electromagnetic field to the matter. This process is reversible, and therefore, it is possible to identify a new state of matter when energy oscillates

between an electromagnetic field and matter.

The process of instant creation and annihilation of the $e-p$ pair would cause randomization of photon momentum; that is, the photon-photon scattering amplitude demonstrates little dependence on the scattering angle. We can imagine the multiphoton state with random photon motion and expansion based on the diffusion equation. The light-in-light diffusion coefficient is shown to be dependent only on fundamental constant $D \sim \alpha^{-2} \hbar/m$. It should be noted that \hbar/m has the dimensions of a diffusion coefficient. It merely describes a new quantum state and is independent of any density, contrary to the case of diffusion of gases or diffusion of charges in solid-state matter. The biphoton state is neither plasma nor light; it is a mix (quantum superposition) of the biphoton and $e-p$ pair and slowly expanding.

A systematic approach to the problem of the state involves the calculation of poles of the exact scattering amplitude. These poles lie off-shell of the one-particle photon state and are responsible for the biphoton state, similar to the case of positronium [6]§125. The pole of the exact scattering amplitude is of diffusion type, similar to the problem of quantum interference in solids.[7] The exact energy of the biphoton quantum state is not defined, because it mixes photons with energies above the $e-p$ pair birth threshold.

The condensation of biphotons in a gapped quantum (BCS-like) state is also possible. One can formulate an equation similar to Gorkov's equation for biphotons and search for the energy gap. It is an accepted view that single photons in free space cannot have an energy gap owing to gauge invariance[8]. Therefore the gapped state is unlikely to exist.

It is suggested that this quantum state can be applied to the theory of ball lightning. In particular, it can explain characteristic (vii), as formulated by Rakov and Uman [9, 10]: “the fact that it [ball lightning] appears to pass through small holes, through metal screens,

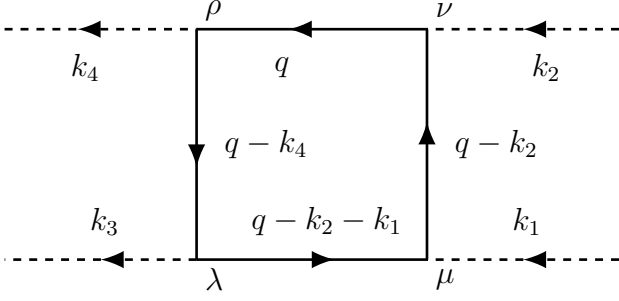


FIG. 1. Photon-photon interaction diagram. Above the e - p pair birth threshold q is the electron, $q - k_2 - k_1$ is the positron, and $q - k_2$ and $q - k_4$ are off-shell fermions. Indexes of the vector potential are either $\mu = \lambda = 0$ and $\nu = \rho = 1, 2, 3$ or $\mu = \lambda = 1, 2, 3$ and $\nu = \rho = 0$.

and through glass windows.” For example, a ball lightning was observed inside an aircraft [11]. Indeed, the conversion of electromagnetic energy into matter occurs through the tunneling of an electron from Dirac’s sea to the real state; it is possible that the electron will simultaneously tunnel through the obstacle, for example, a metal screen. The interaction of the biphoton state with matter is yet to be discussed. On the one hand, this state should have little interaction with matter and be able to pass through metallic or glass screens. On the other hand, the electromagnetic field of this state can ionize the air and create light emission, seen by an observer as a ball lightning.

The process of formation of the new state still needs to be discussed. Experimental evidence [12–17] suggests that a macroscopic amount of e - p pairs should be created by the discharge in a thunderstorm. This explains the discovery of 511-keV annihilation radiation generated by thunderstorms. Simultaneously, the proposed mix state can be formed, not necessarily from the e - p plasma but from the direct transition of the discharge energy to the energy of the biphoton.

This rest of the letter is organized as follows. The introduction section is followed by the calculation of the photon–photon scattering amplitude near $2\hbar\omega = 2mc^2$; it has only a few combinations of allowed 4-indexes and restricts the amount of allowed ladder diagrams. Thereafter, integral equations are derived for the sum of ladder diagrams. This approach appears to be appropriate for determining the exact scattering amplitude. Next, the equations are converted to a form such that the diffusion pole is clearly seen. Thereafter, the letter is concluded. From this point, we will use $\hbar = c = 1$.

From the diagram for the bare photon–photon interaction Fig. (1), we have [6]:

$$\begin{aligned}
 i\tilde{\Gamma}_{\lambda,\rho;\mu\nu}(k_3, k_4; k_1, k_2) &= \text{Tr} \int \frac{d^4q}{(2\pi)^4} (-ie\gamma^\mu) \\
 &\times iG(q - k_2)(-ie\gamma^\nu)iG(q)(-ie\gamma^\rho) \\
 &\times iG(q - k_4)(-ie\gamma^\lambda)iG(q - k_1 - k_2) \quad (1)
 \end{aligned}$$

Near the e - p pair birth threshold $G(q - k_2)$ is off-shell, $G(q)$ is an electron, $G(q - k_4)$ is off-shell, $G(q - k_1 - k_2)$ is a positron. The calculation is straightforward:

$$\begin{aligned}
 i\tilde{\Gamma}_{\lambda,\rho;\mu\nu}(k_3, k_4; k_1, k_2) &= -\frac{e^4}{8\pi} \sqrt{\frac{2(\omega - m)}{m}} \\
 &\times \text{Tr} \frac{1}{4} \gamma^\mu \gamma^\nu (1 + \gamma^0) \gamma^\rho \gamma^\lambda (1 - \gamma^0) \quad (2) \\
 2\omega &= k_{10} + k_{20}, \quad k_1 = (k_{10}, \vec{k}_1), \quad k_2 = (k_{20}, \vec{k}_2) \\
 0 < \omega - m &\ll m, \quad |\vec{k}_1 + \vec{k}_2| \ll m
 \end{aligned}$$

The trace yields -2 for either $\mu = \lambda = 0$ and $\nu = \rho = 1, 2, 3$ or $\mu = \lambda = 1, 2, 3$ and $\nu = \rho = 0$. The scattering amplitude is transforming like the electric field \vec{E} component of the electromagnetic field tensor. This is because the scattering process creates non-relativistic e - p pair; it carries the dipole moment having same transformation properties as the electric field.

There are only six nonzero elements out of 256 in the matrix $i\tilde{\Gamma}_{\lambda,\rho;\mu\nu}$ and this restricts the possible forms of ladder diagrams for the bi-photon. There are two ladders having the same index 0 or 1, 2, 3 along the horizontal lines. We will calculate only the diagram presented in Fig. (2); as the other diagram does not contribute to the pole, we will discuss it later. The summation of the ladder diagram is performed using the integral equation

$$\begin{aligned}
 i\Gamma(k_3, k_2; k_1, k_4) &= i\tilde{\Gamma}(k_3, k_2; k_1, k_4) - \int \frac{d^4k'_1}{(2\pi)^4} \quad (3) \\
 &\times i\tilde{\Gamma}(k_3, k'_2; k'_1, k_4) [-iD(k'_1)] [-iD(k'_2)] i\Gamma(k'_1, k_2; k_1, k'_2) \\
 k'_2 &= k'_1 + k_4 - k_3
 \end{aligned}$$

for the diagram in Fig. (2). The summation over the 4-indexes is omitted because they are preserved along horizontal lines. Eq. (3) have extra negative sign owing to the second fermion loop.

Two major approximations will be used through further calculations. Incoming photons should come with opposite momenta in order to give birth to the e - p pair right above the threshold, $|\vec{k}_4 + \vec{k}'_1| \ll m$, and the same holds for outgoing momenta $|\vec{k}_3 + \vec{k}'_2| \ll m$. The internal biphoton momentum should be slow variable $|\vec{k}_3 - \vec{k}_4| \ll m$, $|\vec{k}'_2 - \vec{k}'_1| \ll m$, and $|\vec{k}_2 - \vec{k}_1| \ll m$. Taking all biphoton vectors approximately aligned to z -axis or \vec{n}_z one can see that

$$\vec{k}_4 \sim \vec{k}_3 \sim m\vec{n}_z \quad \vec{k}'_2 \sim \vec{k}'_1 \sim -m\vec{n}_z \quad \vec{k}_2 \sim \vec{k}_1 \sim m\vec{n}_z,$$

meaning that biphoton is backward scattered (flipped) be every scattering event.

The simplification starts with omitting k_1, k_2 and then omitting the primes in k'_1, k'_2 and substituting $\tilde{\Gamma}$ from Eq. (2) into the integral Eq. (3)

$$\begin{aligned}
 \Gamma(k_3; k_4) &= \tilde{\Gamma}(k_3; k_4) + \frac{e^4}{4\pi} \int \frac{d^4k_1}{(2\pi)^4} \quad (4) \\
 &\times \sqrt{\frac{k_{10} + k_{40} - 2m}{m}} D(k_1) D(k_2) \Gamma(k_1; k_2) \\
 k_2 &= k_1 + k_4 - k_3.
 \end{aligned}$$

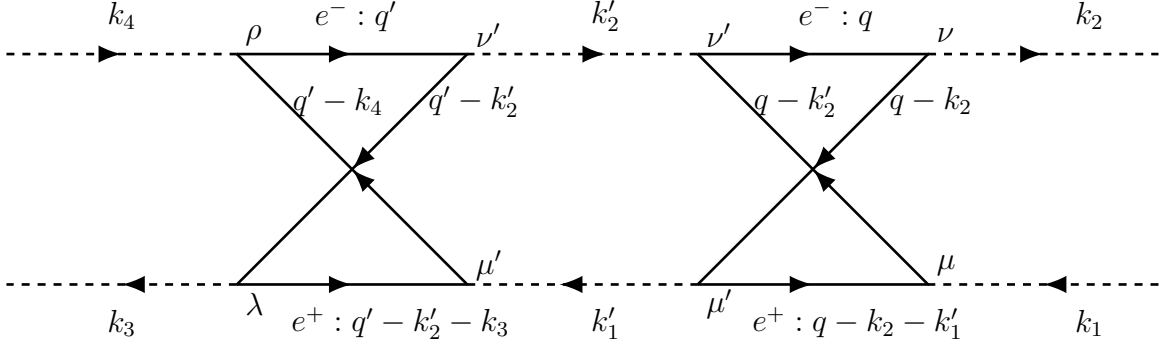


FIG. 2. One of three two-photon ladder diagrams. Electron propagators are marked by e^- , positron propagators are marked by e^+ , this classification is valid above the e - p pair birth threshold. It should be noted that the 4-index is preserved along the upper and lower lines. Specifically, we can substitute $\rho = \nu' = \nu = 1$ or 2 or 3 and $\lambda = \mu' = \mu = 0$ or vice versa.

We multiply both sides of Eq. (4) by $D(k_3)D(k_4)$ and integrate over \vec{k}_3 , where $k_3 \equiv (k_{30}, \vec{k}_3)$. The function $\xi(k_{30}; p)$ will accommodate the left hand side of Eq. (4)

$$\begin{aligned} \xi(k_{30}; p) &= \tilde{\xi}(k_{30}; p) + \frac{e^4}{4\pi} \int \frac{d^3\vec{k}_3}{(2\pi)^3} D(k_3)D(k_3 - p) \\ &\times \int \frac{dk_{10}}{2\pi} \sqrt{\frac{k_{10} + k_{40} - 2m}{m}} \xi(k_{10}; p). \end{aligned} \quad (5)$$

where $p = k_1 - k_2 = k_3 - k_4$. Explicitly the formula

$$\int \frac{d\vec{k}_1}{(2\pi)^3} D(k_1)D(k_1 - p)\Gamma(k_1; k_1 - p) = \xi(k_{10}; p), \quad (6)$$

explains the transformation of the integral in the right hand side of Eq. (4).

We now introduce slow and fast variables; slow variables are of the order of $\omega - m$ and fast variables are of the order of m . The auxiliary function χ is introduced depending on the slow variables Ω, \vec{P} and fast variable ω

$$\begin{aligned} \xi(k_{30}, p) &\equiv \chi(\Omega, \vec{P}, \omega) \\ k_{30} &= \omega + \Omega/2, \quad p = (\Omega, \vec{P}). \end{aligned} \quad (7)$$

The integral over \vec{k}_3 is computed considering that $\xi(k_{10}; p)$ in Eq. (5) is independent of it:

$$\begin{aligned} \int \frac{d^3\vec{k}_3}{(2\pi)^3} D(k_3)D(k_3 - p) &= \int \frac{d^3\vec{k}_3}{(2\pi)^3} \\ &\times \frac{4\pi}{k_{30}^2 - \vec{k}_3^2 + i0} \frac{4\pi}{(p_0 - k_{30})^2 - (\vec{p} - \vec{k}_3)^2 + i0} \\ &= \frac{2\pi}{|\vec{P}|} \tan^{-1} \frac{i\Omega}{|\vec{P}|}, \quad |\Omega|, |\vec{P}| \ll \omega, \end{aligned} \quad (8)$$

which is real when $i\Omega = |\Omega|$. The choice of sign of Ω is consistent with the poles of the photon propagators. The frequency ω is assumed to be a large parameter, and it is eliminated from the final result in Eq. (8).

The simplified integral equation for the diagram presented in Fig. (2), with $k_{10} = \omega' + \Omega/2$, $k_{40} = \omega - \Omega/2$, is as follows:

$$\begin{aligned} \chi(\Omega, \vec{P}, \omega) &= \tilde{\chi}(\Omega, \vec{P}, \omega) + \frac{e^4}{2|\vec{P}|} \tan^{-1} \frac{i\Omega}{|\vec{P}|} \\ &\times \int \frac{d\omega'}{2\pi} \sqrt{\frac{\omega + \omega' - 2m}{m}} \chi(\Omega, \vec{P}, \omega'). \end{aligned} \quad (9)$$

Various approaches were employed to determine the eigenfunctions $\chi_\lambda(\omega)$ and eigenvalues D_λ of the homogeneous part of this equation [with $\tilde{\chi}(\Omega, \vec{P}, \omega) = 0$]:

$$D_\lambda^{-1} \chi_\lambda(\omega) = \frac{e^4}{2} \int_{2m-\omega}^{m+\Lambda} \frac{d\omega'}{2\pi} \sqrt{\frac{\omega + \omega' - 2m}{m}} \chi_\lambda(\omega') \quad (10)$$

The solution is very sensitive to the cutoff Λ in the integral over ω' , which is limited by the validity of Eq. (2). Assuming that the cutoff is $\Lambda \lesssim m$, and D_λ^{-1} is limited by Courant–Fischer–Weyl min–max principle, we have the following estimates:

$$D_\lambda^{-1} \lesssim \frac{e^4}{4\pi^2} \sqrt{\frac{\Lambda^3}{m}}, \quad D_\lambda \gtrsim \alpha^{-2} \frac{\hbar}{m} \approx 2 \times 10^4 \text{ cm}^2/\text{s}. \quad (11)$$

Here, D_λ has been converted back into regular units.

The eigenfunctions $\chi_\lambda(\omega)$ are allowed states of the biphoton in the energy (frequency) space. The biphoton is the mix of pairs of photons with the distribution of frequencies governed by $\chi_\lambda(\omega)$. The eigenvalues $1/D_\lambda$ of the Hermitian operator with kernel $\sqrt{\omega + \omega' - 2m}$ are positive real and provide allowed values of the diffusion coefficient of the biphoton state.

Known eigenfunctions $\chi_\lambda(\omega)$ allows to write the solution to the inhomogeneous integral equation Eq. (9). The exact scattering amplitude $\chi(\Omega, \vec{P}, \omega)$ is now expressed in terms of the function $B(\Omega, \vec{P}; \omega, \omega')$ having expected

poles:

$$\chi(\Omega, \vec{P}, \omega) = \int \frac{d\omega'}{2\pi} B(\Omega, \vec{P}; \omega, \omega') \tilde{\chi}(\Omega, \vec{P}, \omega') \quad (12)$$

$$B(\Omega, \vec{P}; \omega, \omega') = \sum_{\lambda} \chi_{\lambda}(\omega) B_{\lambda}(\Omega, \vec{P}) \chi_{\lambda}(\omega')$$

$$B_{\lambda}(\Omega, \vec{P}) = \left[1 - \frac{1}{D_{\lambda} |\vec{P}|} \tan^{-1} \frac{i\Omega}{|\vec{P}|} \right]^{-1}. \quad (13)$$

The diffusion propagator and the diffusion pole are easily recognizable on long distances, where $D_{\lambda} |\vec{P}| \ll 1$ upon expansion of $\tan^{-1} i\Omega/|\vec{P}| \sim i\Omega/|\vec{P}|$.

The biphoton state calculated here is a quantum object having an energy and dimension scale visible to the naked eye. It is also generated during the high-energy process of interaction of gamma rays with e - p pairs and vacuum. Indeed, the diffusion coefficient of the order of $10^4 \text{cm}^2/\text{s}$ describes a chaotic space object expanding to the size of 100 cm in 1 s.

Two more ladder diagrams, similar to that presented in Fig. (2), have been analyzed, but the connection between the fermionic boxes is arranged in an alternative

way. One of these ladders does not preserve the 4-index along the ladder; therefore, it is actually a double ladder, indicating next-order perturbation in terms of the exponents of α^2 . The third ladder diagram contains an integral over the slow variable $\int d\Omega' \chi(\Omega', \vec{P}, \omega)$ on the RHS of the equation analogous to Eq. (9), and the slow variables are eliminated from the final solution.

In conclusion, a biphoton state that is the quantum superposition of light and matter is reported. It formed near the point where light is backward scattered by the e - p pair. It can be possibly formed by the high concentration of electromagnetic energy, for example, in thunderstorms or in beams of high-power lasers. This state is governed by the diffusion type of the propagator, implying that it can propagate through space without acceleration while expanding constantly. The propagator has six components similar to the electric field in the electromagnetic tensor because the virtual matter state has the symmetry of an electric dipole. The diffusion constant in this propagator depends on basic physical constants such as α , \hbar , m , reflecting the most fundamental nature of the discovered state.

-
- [1] M. Marklund and P. K. Shukla, *Rev. Mod. Phys.* **78**, 591 (2006).
 - [2] Y. Liang and A. Czarnecki, *Canadian Journal of Physics* **90**, 11 (2012), <https://doi.org/10.1139/p11-144>.
 - [3] A. M. Fedotov, N. B. Narozhny, G. Mourou, and G. Korn, *Phys. Rev. Lett.* **105**, 080402 (2010).
 - [4] A. Ejlli, F. Della Valle, U. Gastaldi, G. Messineo, R. Pengo, G. Ruoso, and G. Zavattini, *Physics Reports* **871**, 1 (2020), the PVLAS experiment: A 25 year effort to measure vacuum magnetic birefringence.
 - [5] A. M. Sirunyan (CMS Collaboration), *Physics Letters B* **797**, 134826 (2019).
 - [6] V. Berestetskii, E. Lifshitz, and L. Pitaevskii, *Quantum Electrodynamics, Chap XII* (Butterworth-Heinemann, Oxford, 1982) pp. 501–596.
 - [7] L. Gor'kov, A. Larkin, and D. Khmel'nitskii, *JETP Lett.* **30**, 228 (1979).
 - [8] J. Schwinger, *Phys. Rev.* **82**, 664 (1951).
 - [9] V. Rakov and M. Uman, *Lightning: Physics and Effects* (Cambridge University Press, 2003).
 - [10] M. L. Shmatov and K. D. Stephan, *Journal of Atmospheric and Solar-Terrestrial Physics* **195**, 105115 (2019).
 - [11] R. C. Jennison, *Nature* **224**, 895 (1967).
 - [12] M. S. Briggs, V. Connaughton, C. Wilson-Hodge, R. D. Preece, G. J. Fishman, R. M. Kippen, P. N. Bhat, W. S. Paciasas, V. L. Chaplin, C. A. Meegan, A. von Kienlin, J. Greiner, J. R. Dwyer, and D. M. Smith, *Geophysical Research Letters* **38** (2011).
 - [13] G. J. Fishman, *EOS, Transactions, American Geophysical Union* **92**, 31 (2011).
 - [14] J. R. Dwyer, D. M. Smith, B. J. Hazelton, B. W. Grefenstette, N. A. Kelley, A. W. Lowell, M. M. Schaal, and H. K. Rassoul, *Journal of Plasma Physics* **81**, 475810405 (2015).
 - [15] T. Enoto, Y. Wada, and Y. Furuta, *Nature* **551**, 481–484 (2017).
 - [16] T. Enoto, *Nuclear Physics News* **29**, 22 (2019).
 - [17] P. Kochkin, D. Sarria, C. Skeie, A. P. J. v. Deursen, A. I. d. Boer, C. Allasia, F. Flourens, and N. Østgaard, *J Geophys Res Atmos* **123**, 8074–8090 (2018).

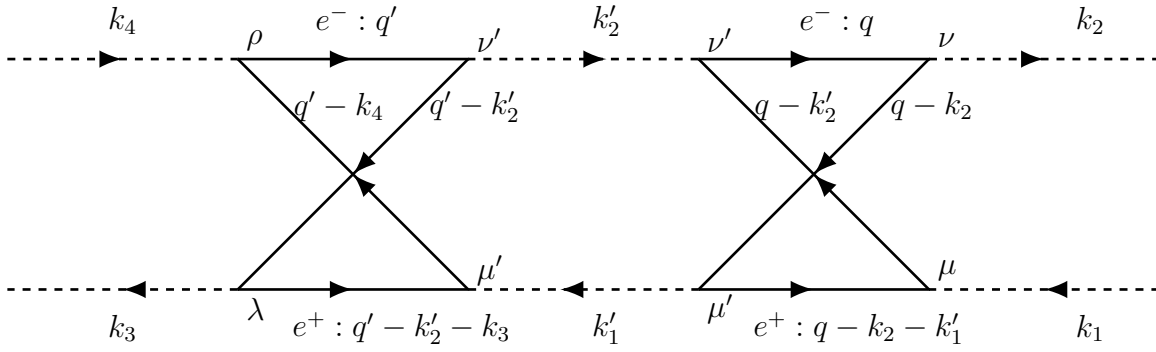


FIG. 3. The bi-photon ladder preserving 4-index along upper and lower lines. We can take $\rho = \nu' = \nu = 1$ or 2 or 3 and $\lambda = \mu' = \mu = 0$ or vice versa. Summation of this ladder is reported in the paper and gives new state with diffusion like pole.

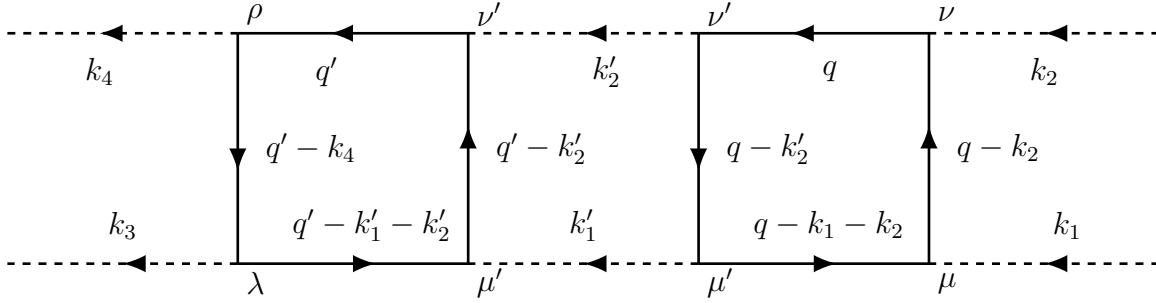


FIG. 4. The bi-photon ladder, please pay attention to 4-index conserved along upper and lower lines. Specifically we can take $\rho = \nu' = \nu = 1$ or 2 or 3 and $\lambda = \mu' = \mu = 0$ or vice versa. Obtained integral equation for the sum of this ladder shows no poles in its solution.

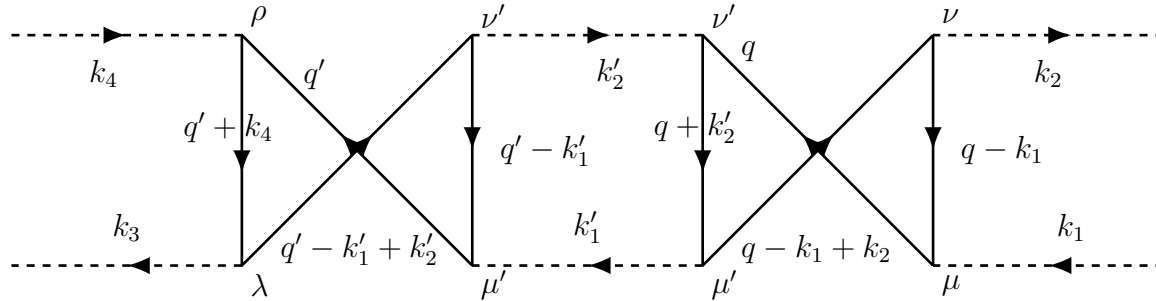


FIG. 5. The bi-photon ladder not preserving 4-index along upper and lower lines. Here $q' + k_4$ and $q + k'_2$ are electrons, $q' - k'_1$ and $q - k_1$ are positrons. We can take $\rho = \lambda = \nu = \mu = 1$ or 2 or 3 and $\mu' = \nu' = 0$. If we take $\rho = \lambda = \nu = \mu = 0$ then summation over $\mu' = \nu'$ gives factor 3. The 4-index summation gives factor 2×3^n for $2n - 1$ fermion blocks in the diagram (starting $n = 1$) and $3^n + 3^{n+1}$ for $2n$ fermion blocks. This ladder summation has no pole too.

I. SUPPLEMENT

Showing again all three diagrams, just for reference.